Radiomic Analysis of Multi-parametric MR Images (MRI) for Classification of Parotid Tumors Running Title: Multi-parametric MRI for Parotid Tumors

Anahita Fathi Kazerooni[1], Mahnaz Nabil[2], Mohammadreza Alviri[3], Soheila Koopaei[3], Faeze Salahshour[4], Sanam Assili[3], Hamidreza Saligheh Rad[1,5], Leila Aghaghazvini[6]*

[1]PhD, Quantitative MR Imaging and Spectroscopy Group, Research Center for Molecular and Cellular Imaging, Tehran University of Medical Sciences, Iran
[2]PhD, Department of Mathematics, Islamic Azad University, Qazvin Branch, Qazvin, Iran
[3]MSc, Quantitative MR Imaging and Spectroscopy Group, Research Center for Molecular and Cellular Imaging, Tehran University of Medical Sciences, Iran
[4]MD, Department of Radiology, Advanced Diagnostic and Invasive Radiology Research Center, Tehran University of Medical Sciences, Tehran, Iran
[5]PhD, Department of Medical Physics and Biomedical Engineering, School of Medicine, Tehran University of Medical Sciences, Iran
[6]MD, Department of Radiology, Shariati Hospital, Tehran University of Medical Sciences, Tehran, Iran

ABSTRACT

Background: Characterization of parotid tumors before surgery using multi-parametric magnetic resonance imaging (MRI) scans can support clinical decision making about the best-suited therapeutic strategy for each patient.

Objective: This study aims to differentiate benign from malignant parotid tumors through radiomics analysis of multi-parametric MR images, incorporating T2-w images with ADC-map and parametric maps generated from Dynamic Contrast Enhanced MRI (DCE-MRI).

Material and Methods: MRI scans of 31 patients with histopathologically-confirmed parotid gland tumors (23 benign, 8 malignant) were included in this retrospective study. For DCE-MRI, semi-quantitative analysis, Tofts pharmacokinetic (PK) modeling, and five-parameter sigmoid modeling were performed and parametric maps were generated. For each patient, borders of the tumors were delineated on whole tumor slices of T2-w image, ADC-map, and the late-enhancement dynamic series of DCE-MRI, creating regions-of-interest (ROIs). Radiomic analysis was performed for the specified ROIs.

Results: Among the DCE-MRI-derived parametric maps, wash-in rate (WIR) and PK-derived K^{trans} parameters surpassed the accuracy of other parameters based on support vector machine (SVM) classifier. Radiomics analysis of ADC-map outperformed the T2-w and DCE-MRI techniques using the simpler classifier, suggestive of its inherently high sensitivity and specificity. Radiomics analysis of the combination of T2-w image, ADC-map, and DCE-MRI parametric maps resulted in accuracy of 100% with both classifiers with fewer numbers of selected texture features than individual images.

Conclusion: In conclusion, radiomics analysis is a reliable quantitative approach for discrimination of parotid tumors and can be employed as a computer-aided approach for pre-operative diagnosis and treatment planning of the patients.

Keywords

Parotid Neoplasms; Radiomics; Texture Analysis; Magnetic Resonance Imaging; Machine Learning; Diagnosis

Introduction

Parotid tumors constitute around 2-3% of head and neck tumors, with diverse histologic subtypes and the majority of the lesions are benign [1]. The most frequently-occurring epithelial benign

*Corresponding author: Leila Aghaghazvini Department of radiology, Shariati hospital . Tehran university of medical sciences, Tehran, Iran
E-mail: aghaghazvini.leila@gmail.com

Received: 9 July 2020
Accepted: 13 November 2020

parotid tumors are pleomorphic adenomas, which if not diagnosed and treated early, can transform to malignant form [2]. Imaging is the cornerstone of diagnosis of parotid gland pathologies, especially for differentiation of inflammatory from neoplastic processes and determining the origin of the pathology [3]. Nonetheless, features based on clinical evaluation and conventional imaging are usually nonspecific and it is difficult to discriminate benign from malignant tumors. Therefore, the requirement for fine needle aspiration cytology (FNAC) for reaching a definitive diagnosis cannot be waived by imaging, and conventional imaging can merely aid to narrow down the possible diagnosis, specify the anatomical extent and guide the biopsy or surgical planning [3, 4]. However, FNAC procedures is an invasive method and susceptible to sampling errors [5], mostly due to intra-tumor heterogeneity of the malignant tumors and their diverse subtypes. This highlights the necessity to adopt advanced methods for pre-operative diagnosis of parotid gland tumors.

In comparison with other imaging methods, standard magnetic resonance imaging (MRI), e.g. T1-wighted (T1-w) and T2-weighted (T2-w) sequences, is the proper method for characterization of parotid gland tumors as it is non-ionizing and provides high soft-tissue contrast [4, 6, 7]. Contrast-enhanced T1-w sequences can indicate the possibility of extra-glandular or perineural spread [6]. It has been suggested that (Fine needle aspiration cytology)FNAC and conventional MRI serve equally to pre-operative characterization of parotid tumors [8]. Nevertheless, conventional MRI lacks sensitivity in predicting tumor malignancy [9].

Diffusion weighted imaging (DWI) is a potent advanced MR imaging method for diagnosis of a variety of tumors [10], such as parotid tumors [2, 4, 6] that has high sensitivity in detecting microstructural changes as it captures microscopic movement of water molecules within the tissue, affected by tissue properties such as the flow between intra- and extra-cellular spaces, perfusion, and structural directionality. In several studies, it has been indicated that apparent diffusion coefficient (ADC) values are significantly lower in malignant as compared to benign lesions, and malignant tumors rarely appear with regions of high ADC-value, whereas pleomorphic adenomas frequently show high ADC values across their expansion [4, 11-16]. I addition, malignant subtypes of parotid tumors such as adenocarcinoma or adenoid cystic carcinoma could have homogeneous appearance on T1-w and T2-w images, however, they indicate heterogeneous manifestation on ADC-maps.

Dynamic contrast-enhanced (DCE-) MRI is another advanced MRI technique that has shown promise in differential diagnosis of parotid gland tumors. The shapes of time intensity curves (TIC) obtained from DCE-MRI are different between benign and malignant tumors [2, 17]. Descriptive parameters of TIC shape, measured by semi-quantitative analysis of TIC, including early enhancement and wash-out rate have been suggested as potent imaging biomarkers for predicting malignancy [9, 18-20]. Four TIC categories have been observed for parotid gland tumors based on time to enhancement peak (*TTP*) and wash-out ratio (*WOR*), where Type 1 is indicative of a flat TIC, Type 2 shows a situation where the TIC has a persistently increasing trend (*TTP*>120 sec), Type 3 occurs with moderate wash-in and persistent to mild wash-out phases (*TTP*≤120 sec & *WOR*≤30%), and Type 4 shows a time intensity curve (TIC) with steep wash-in and wash-out (*TTP*≤120 sec & *WOR*>30%) [17]. While Type 1 and 2 TICs are specific to benign lesions, there exists overlaps between Type 3 and 4 TICs in benign and malignant parotid tumors [18, 21]. Integrating DCE-MRI-derived parameters with ADC-map in a multi-parametric image quantification scheme has demonstrated to improve diagnosis of benign and malignant parotid tumors [17, 21, 22]. Yet, no studies have been carried out on pharmacokinetic (PK) analysis of DCE-MRI in parotid

tumors to determine the capability of the parameters in distinguishing the attributing class of the tumors.

Although DCE-MRI and DWI methods have introduced quantitative approaches to diagnosis of tumors, they are usually acquired with less spatial resolution than conventional T2-w images, which are excellent in detecting the parotid pathologies, their expansion, and their relationship with adjacent anatomical regions. Furthermore, changes in T2 relaxation time of the tissues due to pathogenic alterations across the tumor borders provide helpful parameters for detecting heterogeneity of tumors [23]. Thus, DCE-MRI and DWI should be considered and assessed as additional tools to T2-w MRI.

Quantitative image analysis of tumors through a recently-introduced process, the so-called radiomics analysis approach, can reveal the pathophysiological changes of the heterogeneous tumor tissue through high-dimensional image-derived features [24]. Radiomics analysis has the potential to serve as s for clinical diagnosis of cancers non-invasively and to advance the cancer precision medicine [25]. In parotid tumors, texture analysis of standard T1-w and T2-w images, and ADC-maps, in a univariate approach, for differentiating benign from malignant tumors has been studied by Fruehwald-Pallamar et al. [26], where texture features computed from contrast-enhanced T1-w images were the most and those from T2-w were the least relevant markers for characterizing the tumors.

In the present study, we aimed to tackle the problem of differentiating parotid tumors through radiomics analysis of multi-parametric MR images, incorporating T2-w images with ADC-map and parametric maps generated from DCE-MRI.

Material and Methods

Patients

In this retrospective study, radiomics analysis was performed on a prospectively-acquired dataset of pre-operative MR images of patients with parotid tumors, who underwent surgery within two weeks after MRI and for whom, histopathological assessments were available. Institutional review board (IRB) approval was obtained for retrospective analysis of the data. The patients had provided their informed consent at the time of MR imaging. The database consisted of 41 patients (19 males and 22 females, age range, 13 – 77 years, mean age, 43.1). The database was explored for availability of the whole MR images, including conventional T2-weighted, diffusion-weighted, and dynamic contrast enhanced (DCE) MR images. A total of 31 patients (23 benign, 8 malignant, 15 males, 16 females, age range, 13 – 77 years, mean age, 39.3) with parotid tumors were included in the current study.

MRI Acquisition Parameters

Pre-operative MR imaging of the patients was carried out on a 3T MR scanner (Siemens MAGNETOM Tim TRIO, Erlangen, Germany) using a head coil and a surface coil positioned on the parotid gland. The anatomical sequences comprised of axial T1-weighted (T1-w) imaging with, TE/TR = 11/700 ms, FOV = 200×200 mm^2, matrix size = 205×256, slice thickness = 4 mm, number of slices = 25, and axial T2-weighted (T2-w) imaging with TE/TR = 75/5000 ms, FOV = 200×200 mm^2, matrix size = 307×384, slice thickness = 4 mm, the number of slices = 25. Diffusion-weighted MR imaging (DWI) was performed using 2D spin-echo, single-shot echo-planar imaging with TE/TR = 93/7500 ms, slice thickness = 3.6 mm, FOV = 170×200 mm^2, matrix size = 102×160, number of slices = 25, b-value = 50, 1000 mm^2/s. ADC-maps were automatically generated from DW images on the MRI console. Dynamic contrast-enhanced (DCE) MRI was acquired before and right after injection of 0.2 mL/kg Gd-DTPA followed by 20 cc normal saline with injection rate of 3 mL/min, with the following specifications: TE/TR =

2/5.56 ms, FOV = 220×220 mm^2, matrix size = 256×256, slice thickness = 4 mm, number of slices = 20. The MRI parameters are summarized in Table 1.

Quantification of DCE-MRI

DCE-MR images were quantified based on semi-quantitative approach, Tofts pharmacokinetic (PK) modeling, and five-parameter sigmoid method, using an in-house software, developed in MATLAB 2017b (MathWorks, Inc.). Sigmoid models are empirical mathematical models that can be adapted to fit the DCE-MRI curves. Specifically, five-parameter sigmoid model can best represent the whole trend of TIC curves from the baseline towards wash-in and terminal wash-out phases [27]. From this empirical model, five parameters (P_1 to P_5) are calculated, where $P1$ represents the baseline of the signal, P_2 shows enhancement amplitude of the signal, P_3 denotes the time of maximal slope, P_4 approximates the maximal slope, and P_4 is the terminal enhancement slope [27]. Pixel-wise parametric maps generated from DCE-MRI, consisted of maximum relative signal intensity (SI_{max}), time to peak enhancement (TTP), wash-in-rate (WIR), wash-out-rate (WOR), and area under the enhancement curve (AUEC) from semi-quantitative method, K^{trans}, K_{ep}, and V_e from PK model, and P_1 to P_5 from five-parameter sigmoid model [27].

Region of Interest (ROI) Delineation

For each patient, an experienced radiologist (L.A. with 8 years of experience in head and neck MRI) manually delineated volumetric polygonal whole-lesion borders of the solid portions of parotid lesions throughout the whole slices of T2-w image, ADC-map, and the late-enhancement dynamic series of DCE-MR images. To avoid partial volume effects, the borders were selected immediately inside the outer margin of the lesion. Care was taken to avoid necrotic and cystic areas. The created tumor masks for dynamic image series were overlaid on DCE-MRI parametric maps.

Radiomics Analysis

Conventionally, the analysis of quantitative values in the parametric maps is based on calculation of the average pixel values within the specified ROIs. As tumors are highly heterogeneous, the mean of quantitative values within the ROI could average out this heterogeneity which is a characteristic of the tumors. Alternatively, the region within tumor borders may be characterized using first-order histogram (FOH) analysis that can globally measure the number of pixels with the same quantitative value in the tumor ROI. The descriptive fea-

Table 1: Magnetic Resonance Imaging (MRI) Parameters

	Axial (Pre- and Post-Contrast) T1-w	Axial T2-w	Axial DWI (b-values = 50, 1000)	Axial DCE-MRI
TR (ms)	700	5000	7500	5.56
TE (ms)	10	75	90	2
Flip Angle (º)	120	120	90	12
Field of View (mm²)	220×220	220×220	170×200	220×220
Slice Thickness (mm)	4	4	3.6	4
Matrix	200×256	300×380	100×160	256×256

DWI: Diffusion weighted imaging, DCE: Dynamic Contrast-Enhanced, MRI: Magnetic Resonance Imaging, TR: Repetition Time, TE: Echo Time

tures of the histogram shape are helpful metrics for realizing the variations within the tumor [28]. Yet, FOH analysis cannot consider the interrelationships of local adjacent pixels and it is essential to exploit higher-order statistics, such as gray-level co-occurrence matrix (GLCM) and gray-level run-length matrix (GLRLM), for representing the variations within the tumorous tissue. GLCM method measures the distribution of pixel pairs in a given direction and distance, and GLRLM identifies the coarseness of texture in a specified direction and over a run (a certain amount of consecutive pixels with the same intensity value in a given direction) [29].

In this work, FOH and texture analysis was performed to characterize the parametric maps and T2-w images, show their complementary or competitive value in realizing the heterogeneity within the tumors and facilitate classification of the parotid tumors into benign and malignant categories. A number of features were derived from the specified ROI within the parametric maps and T2-w images (overall n=77 features): (1) first-order histogram (FOH) model (n=10); (2) gray-level co-occurrence matrix (GLCM) (n=23); and (3) gray-level run-length matrix (GLRLM) (n=44) [29]. The textural features were calculated using in-house software developed in MATLAB 2017b (MathWorks, Inc.).

Here, feature selection was applied to the features extracted from each of the DCE-derived parametric maps, ADC-map, and T2-w MRI to assess their diagnostic value for differentiation of parotid tumors. Akaike Information Criterion (AIC) [30] and Schwarz Bayesian Information Criterion (BIC) [31], as statistical information-based feature selection criteria were applied in forward, backward, and stepwise selection approaches, resulting in six feature selection methods to find the best subset of features. For each parametric map or image, the feature subset chosen by the feature selection method that could best approximate the heterogeneity within the parotid tumors, minimize loss of information, and control data overfitting was considered as the desired subset. Leave-one-out cross-validation was performed for feature selection in several iterations (by maintain the number of iterations less than the number of data samples) and the feature subset, which was most frequently selected and generated the highest accuracy, was considered as the desired feature subset representing each image.

Based on the selected feature subsets, classification was performed using Fischer's linear discriminant analysis (LDA) method and support vector machine (SVM) classifier using radial basis functions. Leave-one-out cross-validation was performed in classification to decrease possible effects of outlier samples on the overall diagnostic performance of the classifier. Cross-validation was performed over several iterations of removing a sample and training the model on the whole population minus one sample, and testing the classification on the separated sample. The performance of classification over several iterations of cross-validation was evaluated in terms of sensitivity, specificity, accuracy, and area under the receiver operating (ROC) curve (AUC) metrics. Feature selection and classification were carried out using R Statistical Software (R 3.0.2, Vienna, Austria). The analysis procedure is summarized in Figure 1.

Results

The value of each of the parametric maps generated by DCE-MRI was compared by applying feature selection followed by classification on each of them. The results of radiomics analysis based on LDA and SVM classifiers are summarized in Tables 2 and 3. Here, LDA classifier was applied to determine the inherent potential of a feature subset to predict the attributing class of the disease. According to Table 2, among PK parameters, V_e parameter with a sensitivity of 75%, specificity of 92%, accuracy of 87.3, and AUC of 95%, performs slightly better than K^{trans} and K_{ep}. Among pa-

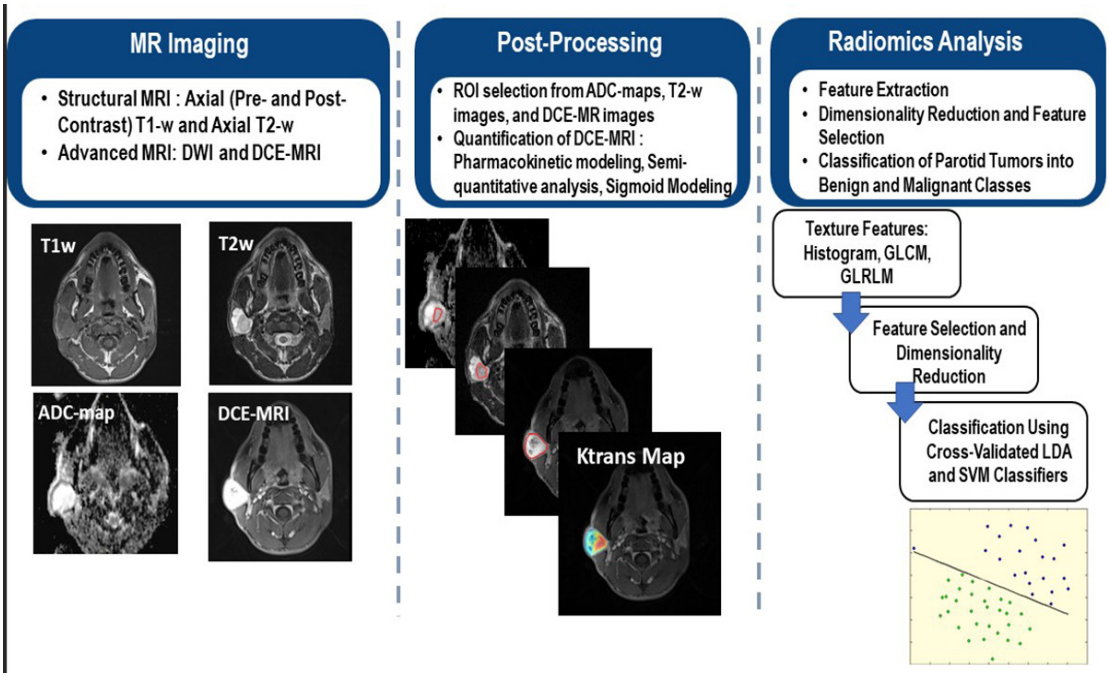

Figure 1: Schematic diagram of the radiomic analysis steps undertaken in this study: (from left to right) after acquisition of magnetic resonance imaging (MRI) scans (structural images: pre- and post-contrast T1-w, and T2-w images; advanced MRI: diffusion weighted imaging (DWI) and dynamic contrast-enhanced (DCE)-MRI; post-processing of the images including quantification of DCE-MRI scans using pharmacokinetic models, semi-quantitative analysis and Sigmoid modeling, and selection of regions of interest (ROIs) from apparent diffusion coefficient (ADC-) maps, T2w images, and quantitative maps derived from DCE-MRI; and finally radiomics analysis including feature extraction, dimensionality reduction and feature selection, and classification of benign and malignant parotid tumors are performed.

rameters calculated by semi-quantitative analysis, *WIR* shows 75% sensitivity, 94% specificity, 89% accuracy, and 94% AUC, and *AUEC* indicates 76% sensitivity, 96% specificity, 91% accuracy, and 97% AUC. Parameters generated by PK modeling and semi-quantitative analysis performed better than five-parameter sigmoid model. The results of SVM classification on feature subsets selected from each DCE-MRI-derived parametric maps are given in Table 3. Using SVM classifier, K^{trans} parameter indicated ~98% sensitivity, 100% specificity, 99.5% accuracy, and 100% AUC, and *WIR* showed a slightly better diagnostic performance with 100% sensitivity, specificity, accuracy, and AUC.

Performance of radiomics analysis on different imaging techniques, i.e. DCE-MRI, ADC-map, T2-w MRI, was compared through applying feature selection followed by LDA and SVM classification on each technique (the results are indicated in Table 4). *ADC*-map classifies the parotid tumors into benign and malignant categories with high diagnostic performance using both LDA and SVM classifiers. The features extracted from DCE-MRI and T2-w revealed comparably high accuracy.

Multi-parametric combination of DCE-MRI, ADC-map, and T2-w images both based on LDA and SVM classifiers induced high diagnostic accuracy and performance (Table 4). The selected features included 95th

Table 2: Radiomics Analysis of Dynamic Contrast Enhanced (DCE-MRI)-Derived Parametric Maps Using Cross-Validated Linear Discriminant Analysis (LDA) Classifier

	Sensitivity (%)	Specificity (%)	Accuracy (%)	AUC (95% CI) (%)
PK Model				
K^{trans}	64.1	95.6	87.5	92.6 (82.8 – 100)
K_{ep}	62.0	96.2	87.4	90.7 (77.9 – 100)
V_e	75.0	91.6	87.3	94.6 (86.9 – 100)
Semi-Quantitative Analysis				
TTP	60.7	99.4	89.5	92.2 (81.1 – 100)
SI_{max}	74.1	94.8	89.5	96.9 (91.6 – 100)
WIR	75.0	94.2	89.2	94.1 (84.6 – 100)
WOR	50.8	92.4	81.7	94.6 (87.0 – 100)
AUEC	75.7	95.8	90.6	96.7 (91.0 – 100)
Five-Parameter Sigmoid Model				
P_1	50.3	98.0	85.7	87.9 (74.8 – 99.9)
P_2	59.4	93.7	84.9	91.3 (79.4 – 100)
P_3	19.1	95.9	76.1	79.2 (60.0 – 98.3)
P_4	35.9	95.5	80.1	84.7 (69.4 – 99.3)
P_5	51.7	91.6	81.3	92.8 (83.8 – 100)

PK: Pharmacokinetic, TTP: Time to enhancement peak, SI: Signal intensity, WIR: Wash-in rate , WOR: Wash-out ratio , AUEC: Area under the enhancement curve, AUC: Area Under the Receiver Operating Characteristic (ROC)

percentile of K^{trans}, maximum, histogram variance (indicating region smoothness), histogram skewness, and 95th percentile of *WIR*, histogram standard deviation, histogram entropy of ADC-map, and few *GLRLM* features from T2-w image.

Discussion

In the current study, through texture analysis of the whole tumors in multi-parametric MR images, we indicated the role of radiomics analysis of different MR imaging techniques, comprising of the parametric maps generated from DCE-MRI, ADC-maps, and T2-w images, in discriminating benign from malignant parotid gland tumors. We showed that by optimizing the radiomics quantification approach, through selection of representative features, and classification, each of these imaging methods could be highly accurate. The most accurate feature set using both LDA and SVM classifiers was the multi-parametric combination of features selected from the three imaging methods. LDA is a nonparametric classifier working by seeking a line that can best discriminate the tumor categories based on the selected features [32]. Thus, since LDA does not require a complicated formulation for separation of data classes like SVM, it may show the inherent discriminative potential of the selected features [29]. Therefore, the information collected from DCE-MRI, DWI, and T2-w are complementary for differentiation of benign from malignant parotid tumors.

Tumors are spatially heterogeneous and undergo regional variations in response to the selection forces [23]. Thanks to its superb contrast resolution, MRI can identify the spatial variations through capturing perfusion alterations by DCE-MRI, cellular density and volume by DWI, and tissue water content by T2-w images. Each of tumor subregions,

Table 3: Radiomics Analysis of Dynamic Contrast Enhanced (DCE-MRI)-Derived Parametric Maps Using Cross-Validated Support Vector Machines (SVM) Classifier (with Radial Basis Functions)

	Sensitivity (%)	Specificity (%)	Accuracy (%)	AUC (95% CI) (%)
PK Model				
K^{trans}	97.7	100	99.5	100 (100)
K_{ep}	79.5	100	94.7	100 (100)
V_e	73.5	100	93.2	100 (100)
Semi-Quantitative Analysis				
TTP	87.9	100	96.9	100 (100)
SI_{max}	75.8	100	93.8	100 (100)
WIR	100	100	100	100 (100)
WOR	87.9	100	96.9	100 (100)
AUEC	87.4	100	96.8	100 (100)
Five-Parameter Sigmoid Model				
P_1	75.8	100	93.7	100 (100)
P_2	63.7	100	90.6	100 (100)
P_3	70.6	100	92.5	100 (100)
P_4	75.4	100	93.7	100 (100)
P_5	87.9	100	96.9	100 (100)

PK: Pharmacokinetic, TTP: Time to enhancement peak, SI: Signal intensity, WIR: Wash-in rate, WOR: Wash-out ratio, AUEC: Area under the enhancement curve, AUC: Area Under the Receiver Operating Characteristic (ROC)

Table 4: Comparison of Radiomics Analysis of Dynamic Contrast Enhanced (DCE-MRI)-Derived Parametric Maps, Apparent Diffusion Coefficient (ADC)-Map, and T2-w Image

	Sensitivity (%)	Specificity (%)	Accuracy (%)	AUC (95% CI) (%)
DCE-MRI				
LDA	86.2	95.4	93.0	99.2 (97.2 – 100)
SVM	100	100	100	100 (100)
ADC-Map				
LDA	100	99.8	99.9	100 (100)
SVM	100	100	100	100 (100)
T2-w Image				
LDA	81.9	93.3	90.4	93.3 (82.1 – 100)
SVM	100	100	100	100 (100)
Multi-Parametric MRI (DCE-MRI, ADC-map, T2-w Image)				
LDA	99.6	100	99.8	100 (100)
SVM	100	100	100	100 (100)

AUC: Area Under the Receiver Operating Characteristic (ROC) Curve, DCE: Dynamic Contrast-Enhanced, MRI: Magnetic Resonance Imaging, LDA: linear discriminant analysis, SVM: Support vector machine, ADC: Apparent Diffusion Coefficient

the so-called tumor habitats, shows different perfusion and diffusion properties, and consequently different responses to the external forces like treatments. Hence, characterization of spatial heterogeneity through integration of diffusion and perfusion imaging along with T2-w MRI and based on texture analysis could aid the pre-operative diagnosis of the patients with parotid tumors and help the clinicians in decision making about the treatment strategy.

As the TIC curve shapes from DCE-MRI could be non-specific in some parotid tumors, it is essential to integrate some other forms of information to increase the diagnostic accuracy. Combination of ADC-map and DCE-MRI in discrimination of parotid gland tumors has been studied by a few groups [17, 21], based on average values computed for the quantitative ADC-map and the derived TICs. Calculating mean of the pixel values in the images averages out the variations of pixel values within the tumor and therefore, the heterogeneity cannot be accounted. Texture analysis overcomes this problem by considering the relationships between the neighboring pixels.

Texture analysis of MR images in parotid tumors has been investigated in a study by Fruehwald-Pallamar et al., where the significance of texture features, derived from T1-w, T2-w and DWI for classifying benign from malignant parotid tumors, was investigated [26]. They suggested that texture analysis of contrast enhanced T1-w (CE-T1w) images have the most relevant classification performance. In the mentioned study, no feature selection methods were applied and the integrative value of the multi-parametric images were not examined. Unlike this study, in our work, we explored the value of radiomics analysis of individual parametric maps generated from DCE-MRI using multiple quantification approaches as well as ADC-maps and T2-w images, in addition to multi-parametric MRI in differentiating parotid gland tumors. Furthermore, CE-T1w images employed in their study, unlike DCE-MRI, cannot detect dynamic alterations of the tumorous region due to neo-angiogenesis and solely provide information about the permeability of tumor vasculature over the late enhancement phase.

Here, we compared three different quantification methods for DCE-MRI, comprising of semi-quantitative, PK modeling, and sigmoid analysis, where the two latter quantification methods have not yet been reported in parotid gland tumors. Five-parameter sigmoid model has the potential to follow the trend of the TIC from the initial to terminal phase [33]. Therefore, it indirectly represents the TIC curve shapes. As mentioned before, the TIC curve shapes have overlaps among benign and malignant tumors since Warthin tumors show somewhat rapid wash-out, similar to malignant tumors [2]. The P_2 and P_5 parameters indicating the wash-in and wash-out phases with 85% and 81% of accuracy based on LDA classifier, respectively, were the best parameters among five-parameter sigmoid model. However, the semi-quantitative parameters, including *WIR* and *AUEC*, showed higher sensitivity compared to P_2 and P_5. Additionally, V_e was comparably accurate based on LDA classifier. By exploiting SVM classifier, K^{trans} and *WIR* features outperformed the other DCE-MRI parametric maps, with approximately 100% accuracy. This demonstrates that by making the classification scheme more effective, the diagnostic performance elevates. By accumulating the features extracted from each of DCE-MRI, ADC-maps, and T2-w techniques and applying SVM, the diagnostic accuracy for each of these techniques improved to 100%. Incorporation of the three imaging techniques could enhance the overall accuracy to around 100% even using LDA classification method. However, this study had a limitation of retrospective design and small patient population.

Combination of DCE-MRI, ADC-maps, and T2-w techniques could better characterize the tumor habitats as each of these methods captures different biophysical or physiological aspects of the tumor region. However, T2-w

images are susceptible to variations among different patients and parameter specifications and DCE-MR imaging has contradictions for some patients. In such situations, given the high diagnostic performance of radiomics analysis of ADC-maps when the machine learning scheme is optimized, independence of DWI from injection, and consistency of ADC-maps among different patients and protocol specifications, radiomics analysis of ADC-maps could be advised.

Conclusion

In conclusion, radiomics analysis is a reliable quantitative approach for discrimination of parotid gland tumors and can be employed as a computer-aided approach for pre-operative diagnosis and treatment planning of the patients. Multi-parametric MRI has the potential for improving the diagnostic performance through integrating various aspects of tumor characteristics.

Acknowledgment

This research has been supported by Tehran University of Medical Sciences & Health Services grant No. 33242.

Conflict of Interest

None

References

1. Lee WH, Tseng TM, Hsu HT, Lee FP, Hung SH, Chen PY. Salivary gland tumors: A 20-year review of clinical diagnostic accuracy at a single center. *Oncol Lett.* 2014;**7**(2):583-7. doi: 10.3892/ol.2013.1750. PubMed PMID: 24396492. PubMed PMCID: PMC3881917.
2. Assili S, Fathi Kazerooni A, Aghaghazvini L, Saligheh Rad HR, Pirayesh Islamian J. Dynamic Contrast Magnetic Resonance Imaging (DCE-MRI) and Diffusion Weighted MR Imaging (DWI) for Differentiation between Benign and Malignant Salivary Gland Tumors. *J Biomed Phys Eng.* 2015;**5**(4):157-68. PubMed PMID: 26688794. PubMed PMCID: PMC4681460.
3. Seifert G. Histopathology of malignant salivary gland tumours. *Eur J Cancer B Oral Oncol.* 1992;**28B**(1):49-56. doi: 10.1016/0964-1955(92)90013-q. PubMed PMID: 1330147.
4. Atkinson C, Fuller J, Huang B. Cross-Sectional Imaging Techniques and Normal Anatomy of the Salivary Glands. *Neuroimaging Clin N Am.* 2018;**28**(2):137-58. doi: 10.1016/j.nic.2018.01.001. PubMed PMID: 29622110.
5. He Y, Zhang ZY, Tian Z. The diagnostic value of fine-needle aspiration cytology (FNAC) for lesions in the parotid gland. *Shanghai Kou Qiang Yi Xue.* 2003;**12**(6):410-3. PubMed PMID: 14966576.
6. Razek AA, Mukherji SK. State-of-the-Art Imaging of Salivary Gland Tumors. *Neuroimaging Clin N Am.* 2018; **28**(2):303-17. doi: 10.1016/j.nic.2018.01.009. PubMed PMID: 29622121.
7. Lee YY, Wong KT, King AD, Ahuja AT. Imaging of salivary gland tumours. *Eur J Radiol.* 2008;**66**(3):419-36. doi: 10.1016/j.ejrad.2008.01.027. PubMed PMID: 18337041.
8. Inohara H, Akahani S, Yamamoto Y, Hattori K, Tomiyama Y, Tomita Y, Aozasa K, Kubo T. The role of fine-needle aspiration cytology and magnetic resonance imaging in the management of parotid mass lesions. *Acta Otolaryngol.* 2008;**128**(10):1152-8. doi: 10.1080/00016480701827533. PubMed PMID: 18607904.
9. Lam PD, Kuribayashi A, Imaizumi A, Sakamoto J, Sumi Y, Yoshino N, Kurabayashi T. Differentiating benign and malignant salivary gland tumours: diagnostic criteria and the accuracy of dynamic contrast-enhanced MRI with high temporal resolution. *Br J Radiol.* 2015;**88**(1049):20140685. doi: 10.1259/bjr.20140685. PubMed PMID: 25791568. PubMed PMCID: PMC4628473.
10. Padhani AR, Miles KA. Multiparametric imaging of tumor response to therapy. *Radiology.* 2010;*256*(2):348-64. doi: 10.1148/radiol.10091760. PubMed PMID: 20656830.
11. Eida S, Sumi M, Sakihama N, Takahashi H, Nakamura T. Apparent diffusion coefficient mapping of salivary gland tumors: prediction of the benignancy and malignancy. *Am J Neuroradiol.* 2007;**28**(1):116-21. PubMed PMID: 17213436.
12. Milad P, Elbegiermy M, Shokry T, Mahmoud H, Kamal I, Taha MS, Keriakos N. The added value of pretreatment DW MRI in characterization of salivary glands pathologies. *Am J Otolaryngol.* 2017;**38**(1):13-20. doi: 10.1016/j.amjoto.2016.09.002. PubMed PMID: 27806890.

13. Takashima S, Sone S, Takayama F, Maruyama Y, Hasegawa M, Horii A, Yoshida J. Assessment of parotid masses: which MR pulse sequences are optimal? *Eur J Radiol.* 1997;**24**(3):206-15. doi: 10.1016/s0720-048x(96)01132-1. PubMed PMID: 9232391.

14. Celebi I, Mahmutoglu AS, Ucgul A, Ulusay SM, Basak T, Basak M. Quantitative diffusion-weighted magnetic resonance imaging in the evaluation of parotid gland masses: a study with histopathological correlation. *Clin Imaging.* 2013;**37**(2):232-8. doi: 10.1016/j.clinimag.2012.04.025. PubMed PMID: 23465973.

15. Habermann CR, Gossrau P, Graessner J, Arndt C, Cramer MC, Reitmeier F, Jaehne M, Adam G. Diffusion-weighted echo-planar MRI: a valuable tool for differentiating primary parotid gland tumors? *Rofo.* 2005;**177**(7):940-5. doi: 10.1055/s-2005-858297. PubMed PMID: 15973595.

16. Kazerooni AF, Assili S, Alviri MR, et al. Accurate Classification of Parotid Tumors Based on Apparent Diffusion Coefficient. *Frontiers in Biomedical Technologies*. 2018;**4**(3-4):90-9.

17. Eida S, Sumi M, Nakamura T. Multiparametric magnetic resonance imaging for the differentiation between benign and malignant salivary gland tumors. *J Magn Reson Imaging*. 2010;**31**(3):673-9. doi: 10.1002/jmri.22091. PubMed PMID: 20187211.

18. Yabuuchi H, Fukuya T, Tajima T, Hachitanda Y, Tomita K, Koga M. Salivary gland tumors: diagnostic value of gadolinium-enhanced dynamic MR imaging with histopathologic correlation. *Radiology*. 2003;**226**(2):345-54. doi: 10.1148/radiol.2262011486. PubMed PMID: 12563124.

19. Hisatomi M, Asaumi J, Yanagi Y, Unetsubo T, Maki Y, Murakami J, et al. Diagnostic value of dynamic contrast-enhanced MRI in the salivary gland tumors. *Oral Oncol*. 2007;**43**(9):940-7. doi: 10.1016/j.oraloncology.2006.11.009. PubMed PMID: 17257881.

20. Eida S, Ohki M, Sumi M, Yamada T, Nakamura T. MR factor analysis: improved technology for the assessment of 2D dynamic structures of benign and malignant salivary gland tumors. *J Magn Reson Imaging*. 2008;**27**(6):1256-62. doi: 10.1002/jmri.21349. PubMed PMID: 18504743.

21. Yabuuchi H, Matsuo Y, Kamitani T, Setoguchi T, Okafuji T, et al. Parotid gland tumors: can addition of diffusion-weighted MR imaging to dynamic contrast-enhanced MR imaging improve diagnostic accuracy in characterization. *Radiology*. 2008;**249**(3):909-16. doi: 10.1148/radiol.2493072045. PubMed PMID: 18941162.

22. Attyé A, Troprès I, Rouchy RC, Righini C, Espinoza S, Kastler A, Krainik A. Diffusion MRI: literature review in salivary gland tumors. *Oral Dis.* 2017;**23**(5):572-5. doi: 10.1111/odi.12543. PubMed PMID: 27422846.

23. Gatenby RA, Grove O, Gillies RJ. Quantitative imaging in cancer evolution and ecology. *Radiology.* 2013;**269**(1):8-15. doi: 10.1148/radiol.13122697. PubMed PMID: 24062559. PubMed PMCID: PMC3781355.

24. Gillies RJ, Kinahan PE, Hricak H. Radiomics: Images Are More than Pictures, They Are Data. *Radiology.* 2016;**278**(2):563-77. doi: 10.1148/radiol.2015151169. PubMed PMID: 26579733. PubMed PMCID: PMC4734157.

25. Wong AJ, Kanwar A, Mohamed AS, Fuller CD. Radiomics in head and neck cancer: from exploration to application. *Transl Cancer Res*. 2016;**5**(4):371-82. doi: 10.21037/tcr.2016.07.18. PubMed PMID: 30627523. PubMed PMCID: PMC6322843.

26. Fruehwald-Pallamar J, Czerny C, Holzer-Fruehwald L, Nemec SF, Mueller-Mang C, Weber M, Mayerhoefer ME. Texture-based and diffusion-weighted discrimination of parotid gland lesions on MR images at 3.0 Tesla. *NMR Biomed.* 2013;**26**(11):1372-9. doi: 10.1002/nbm.2962. PubMed PMID: 23703801.

27. Fathi Kazerooni A, Nabil M, Haghighat Khah H, Parviz S, Gity M, Saligheh Rad H. A one-step biomarker quantification methodology for DCE-MRI of adnexal masses: Capturing kinetic pattern from early to late enhancement. *Magn Reson Med.* 2018;**79**(2):1165-71. doi: 10.1002/mrm.26743. PubMed PMID: 28480550.

28. Just N. Improving tumour heterogeneity MRI assessment with histograms. *Br J Cancer*. 2014;**111**(12):2205-13. doi: 10.1038/bjc.2014.512. PubMed PMID: 25268373. PubMed PMCID: PMC4264439.

29. Fathi Kazerooni A, Nabil M, Haghighat Khah H, Alviri M, Heidari-Sooreshjaani M, Gity M, Malek M, Saligheh Rad H. ADC-derived spatial features can accurately classify adnexal lesions. *J Magn Reson Imaging*. 2018;**47**(4):1061-71. doi: 10.1002/jmri.25854. PubMed PMID: 28901638.

30. Akaike H. Information theory and an extension of the maximum likelihood principle. *Selected*

Papers of Hirotugu Akaike. 1998:199-213.

31. Schwarz G. Estimating the dimension of a model. *The Annals of Statistics.* 1978;**6**(2):461-4. doi: 10.1214/aos/1176344136.
32. Fukunaga K. Introduction to statistical pattern recognition. Elsevier; 2013.
33. Moate PJ, Dougherty L, Schnall MD, Landis RJ, Boston RC. A modified logistic model to describe gadolinium kinetics in breast tumors. *Magn Reson Imaging.* 2004;**22**(4):467-73. doi: 10.1016/j.mri.2004.01.025. PubMed PMID: 15120165.